

## MHD WAVES AT THE PRE-FRONT OF INTERPLANETARY SHOCKS ON SEPTEMBER 6 AND 7, 2017

S.A. Starodubtsev 

*Yu.G. Shafer Institute of Cosmophysical Research  
and Aeronomy SB RAS,  
Yakutsk, Russia, starodub@ikfia.ysn.ru*

L.P. Shadrina 

*Academy of Sciences of the Republic of Sakha,  
Yakutsk, Russia, lushadr@mail.ru*

**Abstract.** We analyze strong space weather disturbances during first ten days of September 2017, using the geomagnetic *Dst* index, parameters of normals to interplanetary shock fronts, direct measurements of interplanetary magnetic field, solar wind, and cosmic ray parameters. By applying spectral analysis methods to interplanetary medium data, we analyze MHD waves at the pre-front of two interplanetary shocks responsible for geomagnetic disturbances on September 6 and 7, 2017. The main results are as follows: the contribution of three branches of MHD waves (Alfvén, fast and slow magnetosonic) to the observed spectrum of the interplanetary magnetic field modulus has been established. We have confirmed the conclusion that the generation of Alfvén waves and fast magnetosonic waves is due to

the presence of low-energy proton fluxes ( $E_p \sim 1$  MeV) at the pre-front of interplanetary shocks. We have also discovered a predominant contribution of slow magnetosonic waves to the observed spectrum of the interplanetary magnetic field modulus, but its reason is yet unknown. It is noted that different orientations of the normals to the interplanetary shock fronts and to the direction of the interplanetary magnetic field average vector on spacecraft located fairly close to each other may indicate waviness of the shock front structure.

**Keywords:** interplanetary magnetic field, solar wind, MHD waves, interplanetary shock, geomagnetic storm, cosmic rays, Forbush decrease.

### INTRODUCTION

The study of space weather is a very important area of research in solar-terrestrial physics at present. These studies are of particular importance for the Far North regions, where different economic sectors are currently intensively developing, and terrestrial negative space weather effects are most pronounced. At the same time, the emphasis is on the study of various interplanetary medium parameters, which change significantly with sudden changes in space weather. In this regard, it should be noted that the solar wind (SW) turbulence is one of the significant space weather factors. Many works concentrate largely on high-amplitude Alfvén waves (AW). It is believed that AW has a significant impact on the development of severe geomagnetic storms and Forbush decreases in galactic cosmic rays (GCRs). There is a view [Borovsky, Funsten, 2003; Borovsky, 2023] that it is the contribution of AW that is one of the main drivers of the interaction between SW and Earth's magnetosphere. The turbulence effect is interpreted as an increase in the viscous interaction between SW streams and the magnetosphere, which, in particular, leads to the development of a geomagnetic storm. Rezeau and Belmont [2001], for example, address the question about penetration of MHD waves into the inner magnetosphere through the magnetopause. In [D'Amicis et al., 2022; Jankovicova et al., 2008], Alfvén turbulence characteristics in fast and slow SW are compared and it is shown that there are Alfvén fluctuations in the streams of both types. A number of papers examine the relationship between MHD turbulence and large-scale SW disturbances — interplanetary coronal mass ejections (CMEs), energetic storm particles, solar energetic particles, and SW corotating interaction regions [Luttrell, 1986, 1987; Luttrell,

Richter, 1987; Starodubtsev et al., 2007; Grigoryev et al., 2008; Desai et al., 2012; Riazantseva et al., 2020; Gololobov et al., 2023].

Here, the term "energetic storm particles" refers to a CR flux with  $E \sim 1$  MeV reflected or accelerated at the front of quasi-parallel interplanetary shocks (IS). The flux of these particles increases by several orders of magnitude relative to the background within  $\sim 1$  day before the arrival of a shock at a recorder and has a maximum at the SW front.

The above works have delved into the power spectra of the interplanetary magnetic field (IMF) and fluctuations in the SW velocity and density in an inertial frequency range above  $\sim 10^{-4}$  Hz, occurring both before and after quasi-parallel fast IS. Yet, the question about the nature, i.e. the mechanism and place of generation of MHD waves, is still not completely clear.

In this regard, the purpose of this work is to elucidate the nature and distribution of MHD waves in the inertial region of the SW turbulence spectrum in the vicinity of IS, which caused significant geophysical effects in early September 2017.

### DATA AND METHOD

As initial data we use 1-hour *Dst* data [[https://wdc.kug.i.kyoto-u.ac.jp/dst\\_provisional/index.html](https://wdc.kug.i.kyoto-u.ac.jp/dst_provisional/index.html)], neutron monitor data from the station Apatity [<http://pgia.ru/cosmicray>] on the intensity of low-energy CRs measured by the WIND spacecraft (SC) [[https://omniweb.gsfc.nasa.gov/ftpbrowser/wind\\_epact\\_step\\_flux\\_hr.html](https://omniweb.gsfc.nasa.gov/ftpbrowser/wind_epact_step_flux_hr.html)], 1 min direct measurements of IMF and SW parameters made by SC WIND and DSCOVR

[[https://omniweb.gsfc.nasa.gov/form/sc\\_merge\\_min.html](https://omniweb.gsfc.nasa.gov/form/sc_merge_min.html)], and average parameters of normals to IS fronts recorded by these two SC [<https://lweb.cfa.harvard.edu/shocks>].

To determine properties of MHD waves in the inertial region of the SW turbulence spectrum in the frequency range  $\sim 10^{-4}$ – $10^{-2}$  Hz, we have employed the method and technique for calculating various spectral characteristics of IMF and SW plasma parameters, detailed in [Starodubtsev et al., 2023].

When identifying MHD waves, we took into account that waves of different types are characterized by correlation (in our case, we applied its analog in the frequency domain — coherence) between certain interplanetary medium parameters. Thus, the coherence between  $B$  and  $U$  is typical of AW and determines their contribution to the observed IMF turbulence spectrum; the coherence between IMF and the SW plasma density  $n$ , of fast magnetosonic (FMS) waves; and the coherence between  $n$  and  $U$  indicates the existence of a certain number of slow magnetosonic (SMS) waves in the interplanetary medium [Toptygin, 1983; Luttrell, 1986, 1987; Luttrell, Richter, 1987].

in early September 2017. The observed space weather changes in Earth's orbit at that time were caused by an increase in sporadic solar flare and coronal activity in active region AR12673. Several powerful flares of X-ray class M and X were recorded in it, which generated solar CRs of low and relativistic energies, as well as CME [<https://umbra.nascom.nasa.gov/SEP>; <https://www.spaceweather.com>]. Various terrestrial responses of this interplanetary disturbance have been discussed from different points of view in many papers (see, e.g., [Bruno et al., 2019; Clilverd et al., 2018; Mishev et al., 2018; Safargaleev, Tereshchenko, 2019; Struminskii et al., 2020; Kravtsova, Sdobnov, 2021; Yakhnin, Yakhnina, 2022; Mostafa et al., 2022; Despirak et al., 2020, 2023; Maksimov et al., 2023].

Some powerful geophysical effects were observed on Earth at this time. Figure 1,  $a$ – $e$  illustrates variations in IMF and SW plasma parameters in near-Earth space ( $a$ – $c$ ), as measured by the WIND spacecraft, and their corresponding manifestations in the geomagnetic field and the GCR intensity ( $d$ ,  $e$ ).

## RESULTS AND DISCUSSION

To achieve this purpose, we have analyzed the strong interplanetary medium disturbances occurring

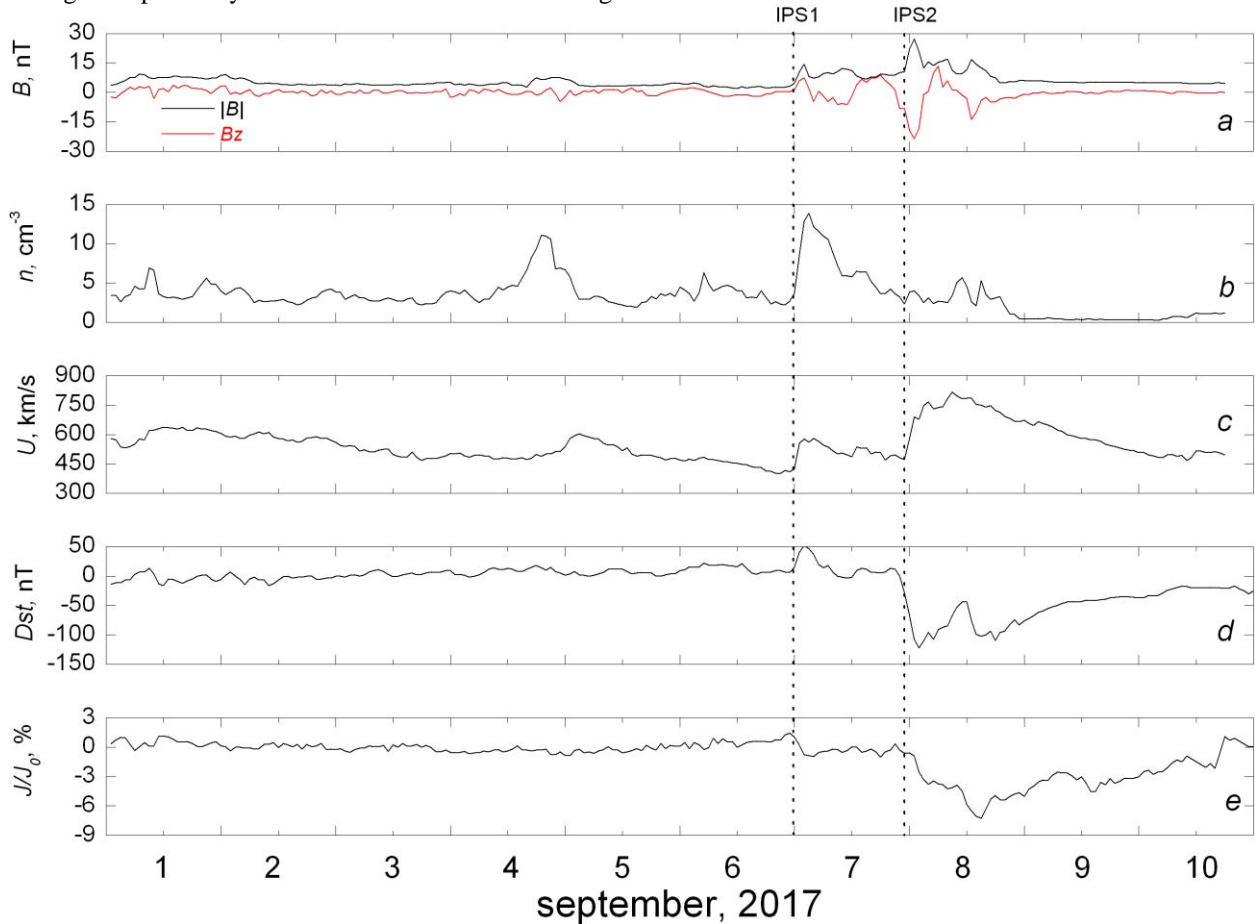


Figure 1. Time dependence of the IMF  $B$  and  $B_z$  component ( $a$ ), SW density ( $b$ ) and velocity ( $c$ ) according to WIND data, as well as  $Dst$  ( $d$ ) and CR intensity ( $e$ ), recorded by the neutron monitor at the CR station Apatity, for September 1–10, 2017. Vertical dashed lines indicate the time of recording of two IS by WIND SC, which were located near the libration point L1

As observed in [Mostafa et al., 2022], on September 6, 2017 at 23:44 UT there was a storm sudden commencement (SSC) (*d*) in the geomagnetic field. It was caused by the arrival of the first interplanetary shock (IS1) (Figure 1, *a-c*). At the same time, *Dst* reached its maximum value of +32 nT at 02:00 UT on September 7, but no magnetic storm ( $Dst < -20$  nT) was recorded (*d*). It is generally accepted that the main reason for the decrease in *Dst* during magnetic storms is a long southward turn of the IMF  $B_z$  component, yet in this case this was not observed. With the arrival of IS2 at Earth at ~21:00 UT on September 7, a large geomagnetic storm began during which *Dst* reached a minimum value of -142 nT within 5 hrs (to ~02:00 UT on September 8). This is due to the fact that the CME that reached Earth's orbit was accompanied by a magnetic cloud (MC) with long and large negative (southward)  $B_z$  (~-20 nT) at the end of September 7. Another MC with minimum  $B_z$  ~-18 nT in the middle of September 8 intensified this geomagnetic storm: *Dst* began to recover, but from 12 to 16 UT decreased again from -63 to -122 nT (panel *d*).

Note that interplanetary CME consists of three parts: IS, plasma compression region behind its front, and MC [Howard, 2011]. The IS is generated by CME itself when it moves at a super-Alfvén velocity relative to the medium. The plasma compression region is a consequence of the interaction of IS with the background SW parameters and features an increased level of their turbulent fluctuations. A magnetic cloud is solar plasma with a frozen-in magnetic field whose field lines look like an expanding loop the ends of which are presumably connected to the solar surface.

During the same period, two Forbush decreases were recorded in the GCR intensity at the CR station Apatity (panel *e*). The beginning of the first one on September 6, 2017 at ~23:00 UT was also caused by the arrival of IS1, and it almost coincided with SSC; in this case, a decrease in the CR intensity was ~2.0 %. The second Forbush effect with a much higher amplitude ~7.5 % began on September 7 at ~22:00 UT (panel *e*). It was also conditioned by the arrival of CME, which occurred with IS2 and MC. This decrease in CRs had a complex multi-stage structure, and the second stage was associated with the passage of MC through Earth's orbit on September 8, 2017 (panels *a-e*). Note also that the sharp increase in the CR intensity in late September 10 is a ground level enhancement in SCRs, known as GLE72 (panel *e*) [Mishev et al., 2018; Kravtsova, Sdobnov, 2021].

Return to the study of the properties of MHD waves at the IS1 and IS2 pre-fronts. Figure 2, *a, b* in the XY plane in the GSE coordinate system schematically shows the positions of DSCOVR and WIND relative to Earth on September 6 and 7, 2017 respectively. Along the axes are distances in Earth radii  $R_E$ . Also indicated is the average direction of the IMF vector projection onto the XY plane (blue line) and normals  $n_{sh}$  to the IS front (red arrow); information is given on the mean angle between them  $\Theta_{Bnsh}$  [https://lweb.cfa.harvard.edu/shocks]. IS1 was recorded by DSCOVR on September 6 at 23:07 UT. It was described as a quasi-perpendicular IS with  $\Theta_{Bnsh}=84.9^\circ$  (*a*). Quasi-perpendicular IS2 ( $\Theta_{Bnsh}=65.1^\circ$ ) was detected on September 7 at 22:28 (*b*). These IS

were also recorded by WIND SC: IS1 on September 6 at 23:02 UT, and it was quasi-parallel with  $\Theta_{Bnsh}=42.1^\circ$  (*a*), and IS2, which also arrived on September 7 at 22:28 UT, was already quasi-perpendicular with  $\Theta_{Bnsh}=64.2^\circ$  (*b*). It is noteworthy that on September 7, quasi-perpendicular IS2 was registered by the two spacecraft relatively close to each other (~50  $R_E$  along the Y-axis and ~25  $R_E$  along the X-axis), whereas on September 6 quasi-perpendicular IS1 was recorded by DSCOVR; and quasi-parallel IS1, by WIND.

When analyzing the mutual arrangement of SC and IS properties for 2000–2014, we have identified 35 similar cases. We believe that this might have been caused either by twist of IMF lines like a rope, or by waviness of the structure of the IS front itself. Borovsky [2020], by examining several papers devoted to statistics on the spatial distribution of locations of current sheets and their orientations, offers a flux-tube or “spaghetti” pattern of the solar wind magnetic structure. The IMF flux tubes are, on average, oriented along the Parker spiral direction. On the other hand, we use the term “waviness” and consider that, unlike most IS models dealing with various physical processes occurring in SW in the plane front approximation, the front itself may in fact have a wavy surface rather than a plane one.

A number of studies have examined the level of IMF turbulence depending on IS properties. For example, Pitna et al. [2016], by analyzing 34 predominantly quasi-perpendicular IS, have shown that the level of fluctuations behind IS fronts increases by almost an order of magnitude as compared to their level before IS fronts, but the authors did not specify the type of MHD turbulence. On the other hand, Luttrell and Richter [1987] found AW in a region before and after quasi-parallel

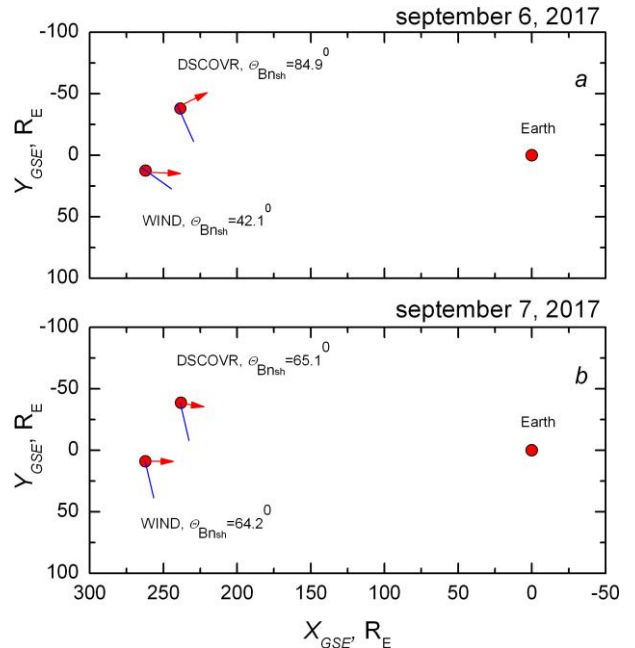


Figure 2. Mutual arrangement of Earth, as well as the DSCOVR and WIND spacecraft in the XY plane (GSE coordinate system) on September 6 (*a*) and 7 (*b*), 2017. Blue segments denote directions of IMF at IS pre-fronts; the red arrows indicate normals to the IS front. Names of the spacecraft and respective angles  $\Theta_{Bnsh}$  are presented

supercritical IS; FMS waves were identified by them upstream from quasi-parallel supercritical IS. Barkhatov et al. [2001] have shown that a low level of turbulence is observed when the IMF direction is perpendicular to the normal to the IS front and the level of turbulence increases during the passage of quasi-longitudinal IS.

To figure out how the SW turbulence behaves and which types of MHD waves are at IS pre-fronts in the case of interest, we have calculated spectral characteristics of the IMF modulus, which contains all the information that is in its components, for two time intervals (1 and 2) at the IS pre-fronts. They are marked with corresponding rectangles 1 and 2 in Figure 3, where SW  $B$ ,  $n$ ,  $U$  recorded by the

DSOVR ( $a-c$ ) and WIND ( $d-f$ ) spacecraft are shown. The power spectra of fluctuations of  $B$  for these two intervals for each spacecraft are exhibited in Figure 4,  $a$ ,  $b$ . The power of IMF fluctuations  $P_{|B|}$  at the IS2 pre-front (solid curves) is seen to be significantly higher than that at the IS1 pre-front (dashed curves). This is quite consistent with the conclusions drawn in [Starodubtsev and Shadrina, 1998], where the turbulence generated before IS is demonstrated to be carried away and redistributed behind the front. This implies that the increased level of turbulence before IS2 serves as a background on which additional turbulence is then generated.

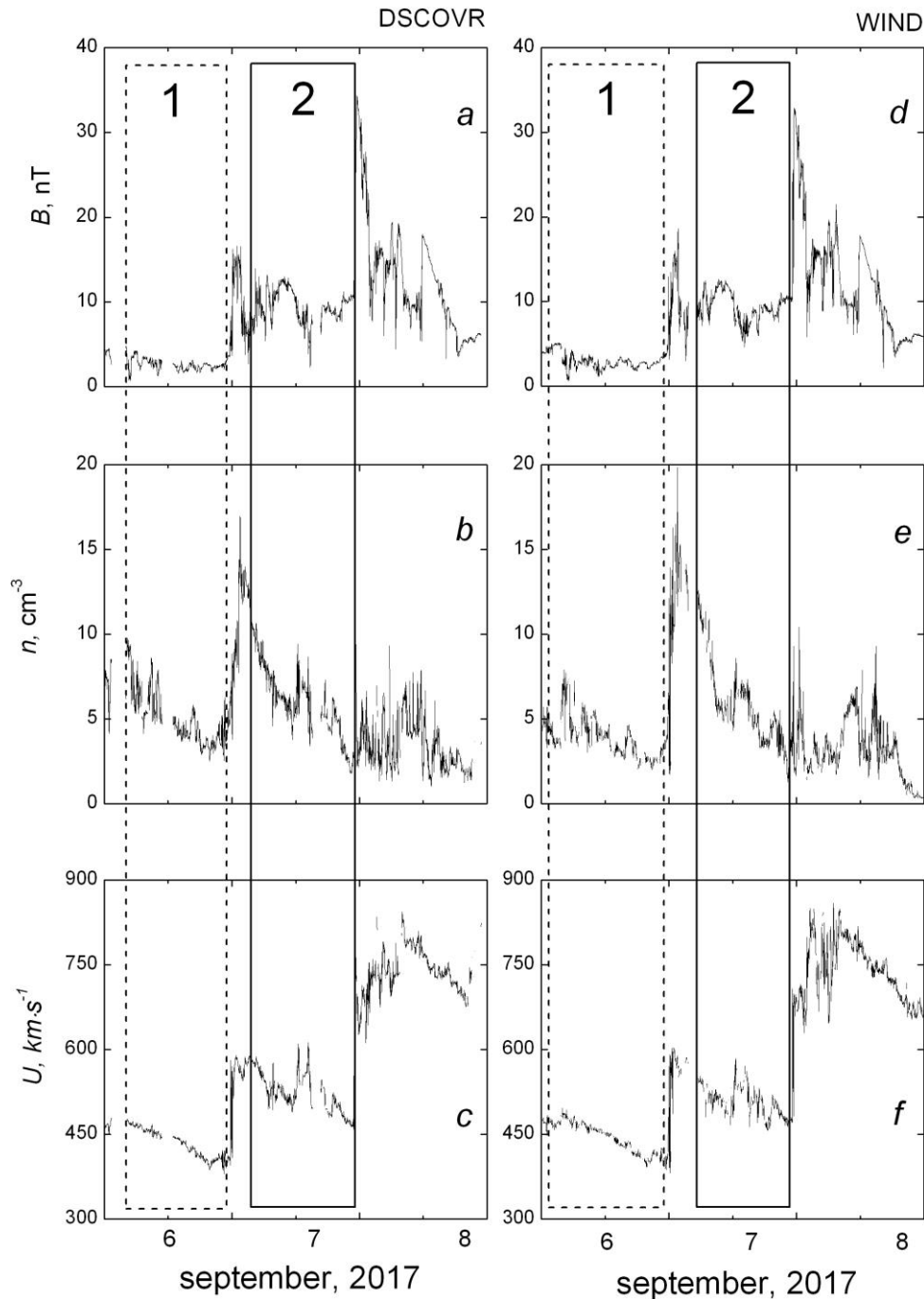


Figure 3. IMF magnitude  $B$ , SW plasma density  $n$  and velocity  $U$  as function of time according to DSCOVR ( $a-c$ ) and WIND ( $d-f$ ) measurements on September 6–7, 2017. Dashed and solid rectangles mark time intervals 1 and 2

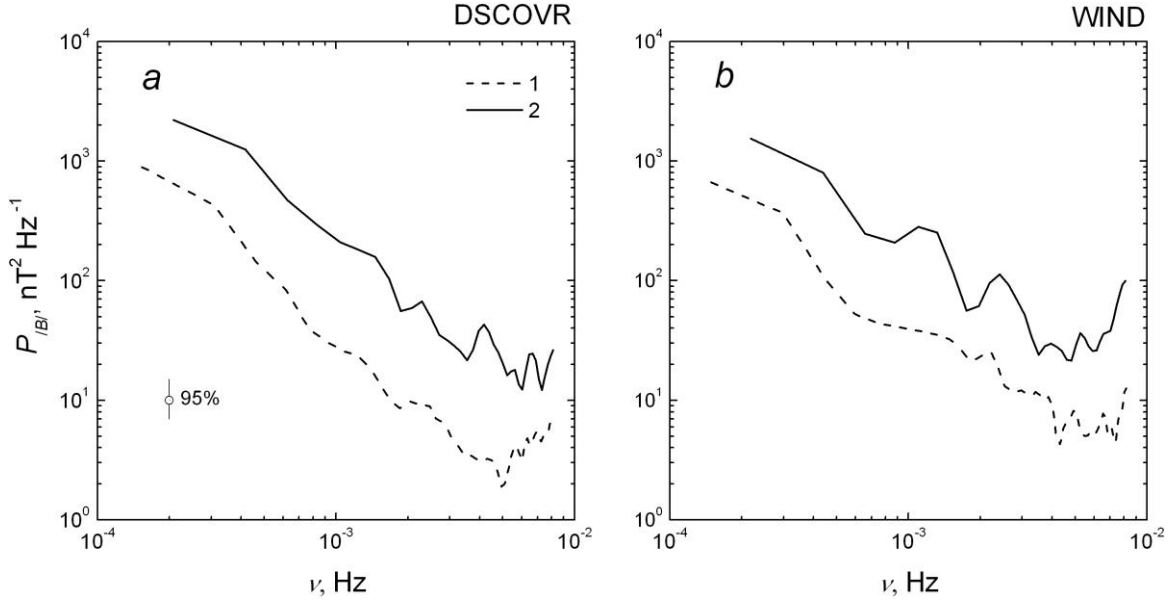


Figure 4. Power spectra of IMF fluctuations as function of frequency according to DSCOVR (a) and WIND (b) data for time intervals 1 and 2. Confidence interval is 95 %

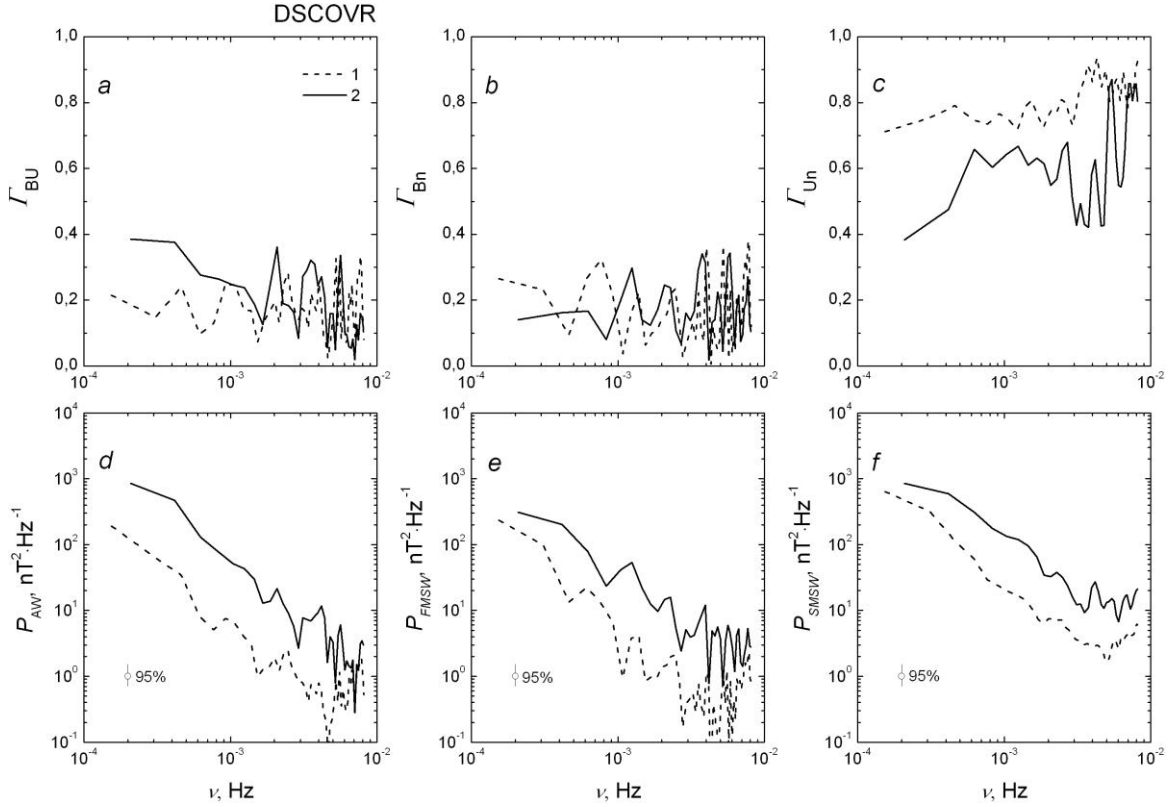


Figure 5. Coherence coefficients  $\Gamma$  between  $B$  and  $U$ ,  $B$  and  $n$ , as well as between  $U$  and  $n$  (a–c) as function of frequency, as well as corresponding power spectra of AW, FMS and SMS waves (d–f) as measured by DSCOVR for time intervals 1 and 2. Confidence intervals are 95 %

The level of MHD-wave turbulence of a certain type can be determined from the coefficients of coherence between IMF and the SW velocity  $\Gamma_{BU}$ , IMF and the SW density  $\Gamma_{Bn}$ , SW velocity and density  $\Gamma_{Un}$  [Starodubtsev et al., 2023 and references therein]. They define the contribution of MHD waves of a certain type to the observed turbulence spectra of IMF, which contains information about waves of all types, oscillations and dis-

continuities always present in SW plasma.

The corresponding calculation results based on DSCOVR and WIND data are presented in Figures 5, a–f and 6, a–f respectively. They indicate that in the time intervals considered the contribution of SMS waves prevails in the observed turbulence spectrum, as evidenced by the coherence coefficients (see Figures 5, a–c and 6, a–c). In the IS1 pre-front on DSCOVR (Figure 5, c), the contribution

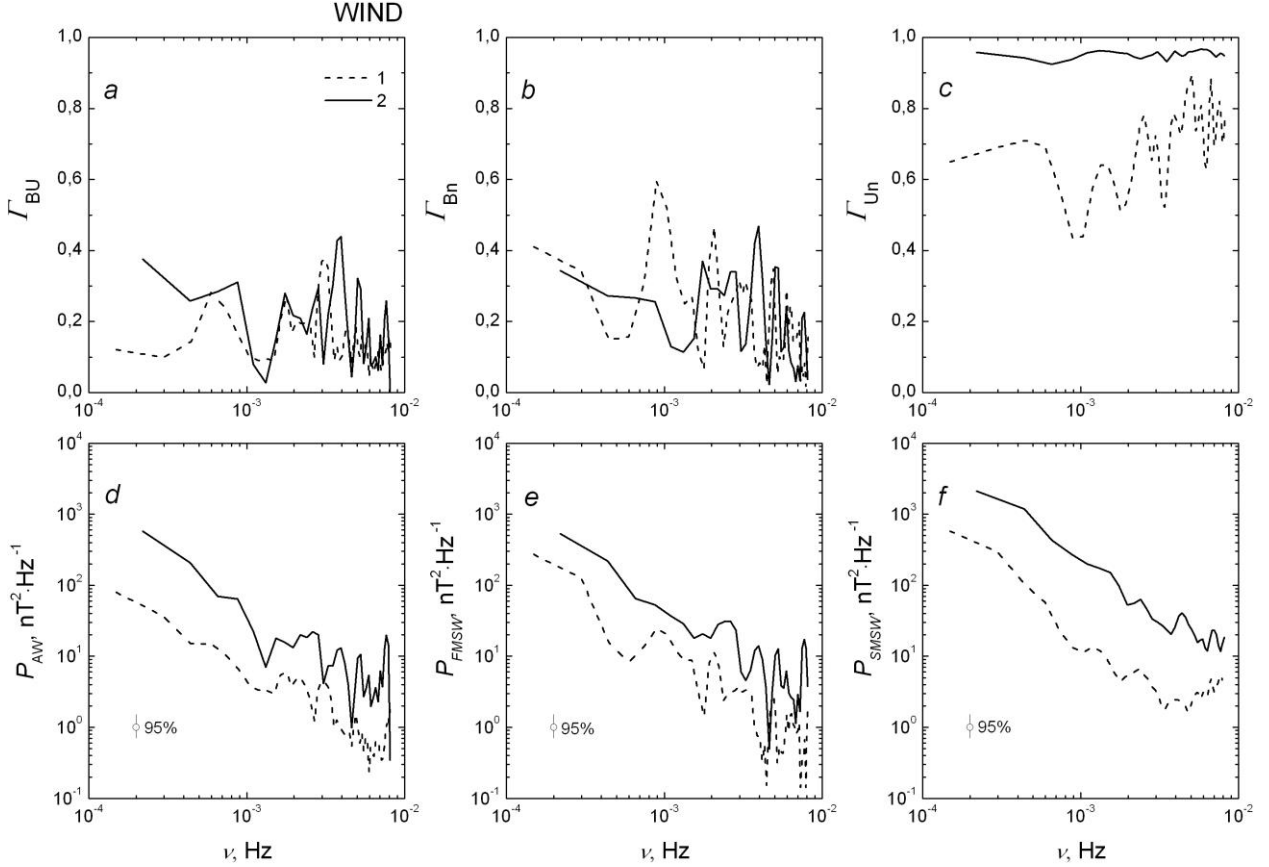


Figure 6. The same for WIND measurements

of SMS waves to the observed IMF power spectrum varies from 70 to  $\sim 90$  % depending on frequency; and for the IS2 pre-front, from 40 to  $>80$  %. On WIND (Figure 6, c) for the first time interval, their number varies from 40 to  $\sim 90$  %; for the second, their contribution is  $\sim 100$  % for all frequencies. Such a significant predominance of the contribution of SMS waves over the rest in the observed IMF power spectra turned out to be a big surprise for us. The reason for this remains unknown, and further detailed studies on a large statistical material are required to uncover it. At present, however, one thing is clear: since, unlike AW, MS waves feature large damping decrements and cannot propagate over long distances, FMS and SMS waves must be generated locally in SW in the direction toward the Sun near Earth's orbit at a distance to 0.2–0.3 AU from the place of their observation.

On the other hand, the coherence coefficients characterizing AW and FMS waves in both cases (see Figures 5, a, b and 6, a, b) are quite low and do not exceed 40–50 % at some frequencies. Only in region 1 at the IS1 pre-front as measured by WIND at a frequency of  $10^{-3}$  Hz  $\Gamma_{Bn}$  reaches 60 %, which may be caused by the presence of storm particles in this region of space.

If we now multiplied the observed power spectra of  $|B|$  fluctuations in time intervals 1 and 2 (see Figure 3) by the corresponding coherence coefficients (see Figures 5, a–c and 6, a–c), it would be easy to calculate the power spectra of fluctuations of all three MHD wave branches, which are recorded in near-Earth space by both spacecraft [Berezhko, Starodubtsev, 1988]. The corresponding power

spectra for MHD waves of each type are exhibited in Figures 5, d–f and 6, d–f. If we put them together, we should ideally get the power spectrum  $|B|$ . This is illustrated in Figure 7, a, b. For interval 1 there are spectra of MHD waves of each type we have identified, their sum, and the observed power spectrum of  $|B|$  fluctuations. The sum  $\Sigma$  of spectra of MHD waves of three types (AW, FMSW, and SMSW) within the 95 % interval is seen to agree well with the observed spectra of  $|B|$ . This proves the correctness of the method, we apply, of identifying spectra of MHD waves of a certain type by analyzing SC data on interplanetary medium parameters. We attribute the small discrepancies between the total spectra of MHD waves and the observed power spectra of  $|B|$  to the oscillations and discontinuities frozen in SW plasma, which always exist in the interplanetary medium and are transferred along with SW from their source to the observation point.

Note that it is almost impossible to visually distinguish between oscillations and waves in observations. Unlike waves, oscillations are static structures frozen in SW and transferred together with it in space, whereas waves have their own velocity relative to SW and can propagate in it both upstream and downstream. In other words, MHD waves, unlike oscillations, are characterized by the presence of a wave vector whose parameters can be determined, for example, by applying the methods of direction cosines and spectral analysis to direct measurements of IMF components [Starodubtsev et al., 2023].

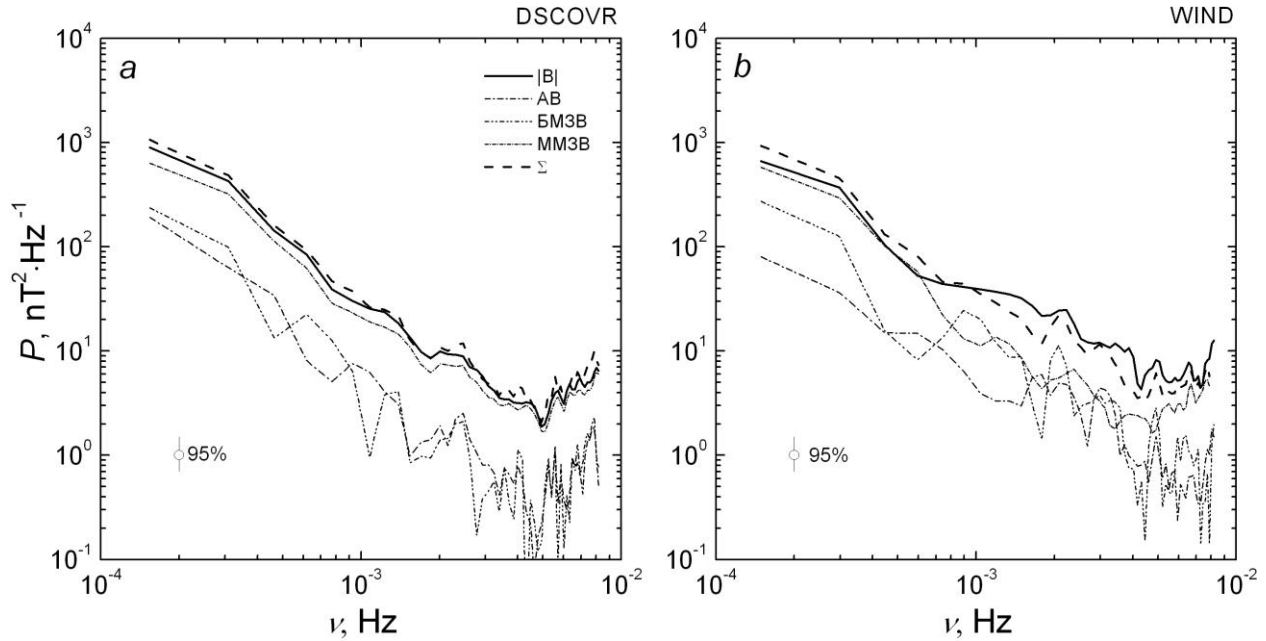


Figure 7. Power spectra of  $|B|$ , AW, FMS and SMS waves, as well as their sum  $\Sigma$  as measured by DSCOVR (a) and WIND (b) for time interval 1. Confidence intervals are 95 %

## CONCLUSIONS

Thus, the analysis allows us to draw the following conclusions.

1. We have identified the contribution of three branches of MHD waves (AW, FMS and SMS waves) to the observed power spectrum of IMF at IS pre-fronts recorded by DSCOVR and WIND, located near the libration point L1 on September 6 and 7, 2017.

2. In the events under study at the IS pre-fronts the predominant contribution of SMS waves to the observed power spectra of  $|B|$  has been found. The reason for this remains unknown. Taking into account the damping decrement of MHD waves of different types, it is clear that SMS waves should be generated locally in SW near Earth's orbit. We assume that entropy waves may play a certain role in this.

3. It is possible that the observation of differently oriented angles between the normals to the front and the direction of the mean IMF vector in the same event of recording of IS passage by SC located relatively close to each other can serve as evidence of the wavy structure of IS fronts or the spaghetti-type structure of IMF.

We are grateful to the teams of the DSCOVR and WIND spacecraft, the Space Weather Prediction Center of the National Oceanic and Atmospheric Administration, and NASA/Goddard Space Flight Center, as well as the Apatity CR stations for free access to measurement data on interplanetary medium and cosmic ray parameters.

We also acknowledge the assistance of the Editorial Board of the journal *Solar-Terrestrial Physics* and the help of Kulish O.A. in preparing the English version of the paper.

The work was performed under Government assignment of the Ministry of Science and Higher Education of the Russian Federation for SHICRA SB RAS

(FWRS-2021-0012) and Government assignment of AN RS (Ya) (Order of the Ministry of Science and Higher Education RS(Ya) No. 01-03/32 dated January 01, 2023).

## REFERENCES

- Barkhatov N.A., Belliustin N.S., Bougeret J.-L., Sakharov S.Yu., Tokarev Yu.V. Influence of the solar-wind magnetic field on the magnetosheath turbulence behind the bow shock. *Radiophysics and Quantum Electronics*. 2001, vol. 44, no. 12, pp. 915–923.
- Berezhko E.G., Starodubtsev S.A. Nature of the dynamics of the cosmic-ray fluctuation spectrum. *Bull. Academy of Sciences of USSR. Ser. Physics*. 1988, vol. 52, pp. 2361–2363 (In Russian).
- Borovsky J.E. What magnetospheric and ionospheric researchers should know about the solar wind. *J. Atmos. Solar Tag. Phys.* 2020, vol. 204, 105271. DOI: [10.1016/j.jastp.2020.105271](https://doi.org/10.1016/j.jastp.2020.105271).
- Borovsky J.E. Further investigation of the effect of upstream solar-wind fluctuations on solar-wind/ magnetosphere coupling: Is the effect real? *Front. Astron. Space Sci.* 2023, vol. 9, 17 p. DOI: [10.3389/fspas.2022.975135](https://doi.org/10.3389/fspas.2022.975135).
- Borovsky J.E., Funsten H.O. Role of solar wind turbulence in the coupling of the solar wind to the Earth's magnetosphere. *J. Geophys. Res.* 2003, vol. 108, p. 1246. DOI: [10.1029/2002JA009601](https://doi.org/10.1029/2002JA009601).
- Bruno A., Christian E.R., de Nolfo G.A. Spectral analysis of the September 2017 solar energetic particle events. *Space Weather*. 2019, vol. 17, pp. 419–437. DOI: [10.1029/2018SW002085](https://doi.org/10.1029/2018SW002085).
- Ciliverd M.A., Rodger C.J., Brundell J.B., Dalzell M., Martin I., Mac Manus D.H., et al. Long-lasting geomagnetically induced currents and harmonic distortion observed in New Zealand during the 7–8 September 2017 disturbed period. *Space Weather*. 2018, vol. 16, pp. 704–717. DOI: [10.1029/2018SW001822](https://doi.org/10.1029/2018SW001822).
- D'Amicis R., Perrone D., Vell M., Sorriso-Valvo L., Teloni D., Bruno R., De Marco R. Investigating Alfvénic turbulence in fast and slow solar wind streams. *Universe*. 2022, vol. 8, p. 352. DOI: [10.3390/universe8070352](https://doi.org/10.3390/universe8070352).

- Desai M., Dayeh M., Ebert R., Smith C., Mason G., Li G. Ion acceleration at CME-driven shocks near the Earth and the Sun. *Proc. IP Conf.* 2012, vol. 1500, iss. 1, pp. 80–85. DOI: [10.1063/1.4768748](https://doi.org/10.1063/1.4768748).
- Despirak I.V., Kleimenova N.G., Gromova L.I., Gromov S.V., Malysheva L.M. Supersubstorms during storms of September 7–8, 2017. *Geomagnetism and Aeronomy.* 2020, vol. 60, no. 3, pp. 292–300. DOI: [10.1134/S0016793220030044](https://doi.org/10.1134/S0016793220030044).
- Despirak I.V., Setsko P.V., Sakharov Ya.A., Lubchich A.A. Geomagnetically induced currents during supersubstorms on September 7–8, 2017. *Bulletin of the Russian Academy of Sciences: Physics.* 2023, vol. 87, no. 7, pp. 999–1006. DOI: [10.3103/S1062873823702283](https://doi.org/10.3103/S1062873823702283).
- Gololobov P., Starodubtsev S., Grigoryev V., Zverev A. NMDB and space weather forecasting. *Cosmic ray studies with neutron detectors.* 2023, vol. 2, pp. 69–80. DOI: [10.38072/2748-3150/p32](https://doi.org/10.38072/2748-3150/p32).
- Grigoryev A.V., Starodubtsev S.A., Grigoryev V.G., Usoskin I.G., Mursula K. Fluctuations of cosmic rays and IMF in the vicinity of interplanetary shocks. *Adv. Space Res.* 2008, vol. 41, pp. 955–961. DOI: [10.1016/j.asr.2007.04.044](https://doi.org/10.1016/j.asr.2007.04.044).
- Howard T. Coronal Mass Ejections: An Introduction. Astrophysics and Space Science Library. Springer Science+Business Media, LLC. 2011, vol. 376. DOI: [10.1007/978-1-4419-8789-1](https://doi.org/10.1007/978-1-4419-8789-1).
- Jankovicova D., Voros Z., Simkanin J. The influence of solar wind turbulence on geomagnetic activity. *Nonlinear Processes Geophys.* 2008, vol. 15, pp. 53–59.
- Kravtsova M.V., Sdobnov V.E. Ground-Level Enhancement in the Intensity of Cosmic Rays during the Decay Phase of Solar Cycle 24: Spectra and Anisotropy. *Bull. Russian Academy of Sciences: Physics.* 2021, vol. 85, no. 8, pp. 919–921. DOI: [10.3103/S1062873821080128](https://doi.org/10.3103/S1062873821080128).
- Luttrell A.H. Power spectra of low frequency MHD turbulence up- and downstream of interplanetary fast shocks within 1 AU. *Ann. Geophys.* 1986, vol. 4, pp. 439–446.
- Luttrell A.H. Evidence for Slow Mode MHD Turbulence in the Solar Wind: Post-Shock Observations at 0.31 AU. *J. Geophys. Res.* 1987, vol. 92, pp. 13653–13657.
- Luttrell A.H., Richter A.K. Study of MHD fluctuations upstream and downstream of quasiparallel interplanetary shocks. *J. Geophys. Res.* 1987, vol. 92, pp. 2243–2252.
- Maksimov D.S., Kogogin D.A., Nasyrov I.A., Zagretdinov R.V. Effects of September 5–12, 2017 solar flares on regional disturbance of Earth’s ionosphere as recorded by GNSS stations located in the Volga Federal District of the Russian Federation. *Solar-Terr. Phys.* 2023, vol. 9, iss. 2, pp. 48–54. DOI: [10.12737/stp-92202306](https://doi.org/10.12737/stp-92202306).
- Mishev A., Usoskin I., Raukunen O., Paassilta M., Valtonen E., Kocharov L., Vainio R. First analysis of ground-level enhancement (GLE72) on 10 September 2017: Spectral and anisotropy characteristics. *Solar Phys.* 2018, 293:136. DOI: [10.1007/s11207-018-1354-x](https://doi.org/10.1007/s11207-018-1354-x).
- Mostafa N., Ghamry E., Ellithi A., Gobashy M., Fathy A. Multi-space observations of the storm sudden commencement (September 2017) and its effect on the geomagnetic field. *Adv. Space Res.* 2022, vol. 70, pp. 641–651. DOI: [10.1016/j.asr.2022.04.023](https://doi.org/10.1016/j.asr.2022.04.023).
- Pitna A., Safrankova J., Nemcek Z., Goncharov O., Němec F., Přech L., et al. Density fluctuations upstream and downstream of interplanetary shocks. *Astrophys. J.* 2016, vol. 819, pp. 41–50. DOI: [10.3847/0004-637X/819/1/41](https://doi.org/10.3847/0004-637X/819/1/41).
- Rezeau L., Belmont G. Magnetic turbulence at the magnetopause, a key problem for understanding the solar wind/magnetosphere exchanges. *Space Sci. Rev.* 2001, vol. 95, pp. 427–441.
- Riazantseva M.O., Rakhmanova L.S., Yermolaev Yu.I., Lodkina I.G., Zastenker G.N., Chesalina L.S. Characteristics of turbulent solar wind in plasma compression regions flow. *Cosmic Res.* 2020, vol. 58, no. 6, pp. 468–477. DOI: [10.1134/S001095252006009X](https://doi.org/10.1134/S001095252006009X).
- Safargaleev V.V., Tereshchenko P.E. Hertz range pulsations during recovery phase of the magnetic storm on September 7–8, 2017, and relation between their dynamics and changes in the parameters of the interplanetary medium. *Geomagnetism and Aeronomy.* 2019, vol. 59, no. 3, pp. 281–295. DOI: [10.1134/S0016793219030125](https://doi.org/10.1134/S0016793219030125).
- Starodubtsev S.A., Grigoriev A.V., Grigoriev V.G., Usoskin I.G., Mursula K. Fluctuations of cosmic rays and IMF in the vicinity of interplanetary shock wave fronts. *Bull. Russian Academy of Sciences: Physics.* 2007, vol. 71, no. 7, pp. 991–993. DOI: [10.3103/S1062873807070295](https://doi.org/10.3103/S1062873807070295).
- Starodubtsev S.A., Shadrina L.P. Distribution of MHD turbulence in the vicinity of the leading front of large-scale solar wind disturbances. *Geomagnetism and aeronomy.* 1998, vol. 38, pp. 9–15 (In Russian).
- Starodubtsev S.A., Zverev A.S., Gololobov P.Yu., Grigoryev V.G. Cosmic ray fluctuations and MHD waves in the solar wind. *Solar-Terr. Phys.* 2023. Vol. 9. Iss. 2. P. 73–80. DOI: [10.12737/stp-92202309](https://doi.org/10.12737/stp-92202309).
- Struminskii A.B., Grigor’eva I.Yu., Logachev Yu.I., Sadovskii A.M. Solar electrons and protons in the events of September 4–10, 2017 and related phenomena. *Plasma Physics Reports.* 2020, vol. 46, no. 2, pp. 174–188. DOI: [10.1134/S1063780X20020130](https://doi.org/10.1134/S1063780X20020130).
- Toptygin I.N. *Cosmic Rays in Interplanetary Magnetic Fields.* Moscow, Nauka Publ., 1983, 304 p. (In Russian).
- Yahnin A.G., Yahnina T.A. 1 MeV Electron dynamics in the outer radiation belt during geomagnetic storms on September 7–8, 2017. *Bull. Russian Academy of Sciences: Physics.* 2022, vol. 86, no. 3, pp. 275–280. DOI: [10.3103/S1062873822030273](https://doi.org/10.3103/S1062873822030273).  
URL: [https://wdc.kugi.kyoto-u.ac.jp/dst\\_provisional/index.html](https://wdc.kugi.kyoto-u.ac.jp/dst_provisional/index.html) (accessed January 21, 2024).  
URL: <http://pgia.ru/cosmicray> (accessed January 21, 2024).  
URL: [https://omniweb.gsfc.nasa.gov/ftpbrowser/wind\\_epact\\_step\\_flux\\_hr.html](https://omniweb.gsfc.nasa.gov/ftpbrowser/wind_epact_step_flux_hr.html) (accessed January 21, 2024).  
URL: [https://omniweb.gsfc.nasa.gov/form/sc\\_merge\\_min1.html](https://omniweb.gsfc.nasa.gov/form/sc_merge_min1.html) (accessed January 21, 2024).  
URL: <https://lweb.cfa.harvard.edu/shocks> (accessed January 21, 2024).  
URL: <https://umbra.nascom.nasa.gov/SEP> (accessed January 21, 2024).  
URL: <https://www.spaceweather.com> (accessed January 21, 2024).

*This paper is based on material presented at the 19th Annual Conference on Plasma Physics in the Solar System, February 5–9, 2024, IKI RAS, Moscow.*

Original Russian version: Starodubtsev S.A., Shadrina L.P., published in *Solnechno-zemnaya fizika.* 2024. Vol. 10. No. 3. P. 53–61. DOI: [10.12737/szf-103202406](https://doi.org/10.12737/szf-103202406). © 2024 INFRA-M Academic Publishing House (Nauchno-Izdatelskii Tsentr INFRA-M)

#### How to cite this article

Starodubtsev S.A., Shadrina L.P. MHD waves at the pre-front of interplanetary shocks on September 6 and 7, 2017. *Solar-Terrestrial Physics.* 2024. Vol. 10. Iss. 3. P. 50–57. DOI: [10.12737/stp-103202406](https://doi.org/10.12737/stp-103202406).